IJHSR
ijhighschoolresearch.org
RESEARCH ARTICLE

Structural Performance of Angled Stringers in FishBAC Morphing Wing

Derin Bahşiş[1], Zehra S. Şentürk[2,3]

1) The Koc School, Tepeören Mahallesi Eski Ankara Asfaltı Caddesi No: 60, Istanbul, 34959, Türkiye; bahsisderin@gmail.com
2) Baykar Technology, Hadımköy-İstanbul Caddesi No:258, Orhan Gazi Mahallesi, Esenyurt, 34538, Istanbul, Türkiye
3) Department of Aeronautical and Astronautical Engineering, Istanbul Technical University, Maslak, 34469, Istanbul, Türkiye; zehrasena.senturk@baykartech.com
Mentor: Gamze Kaynak

ABSTRACT: Leveraging bioinspired design principles, this study evaluates the structural performance of angled stringers (60° orientation) within a FishBAC (Fish Bone Active Camber) morphing wing. Morphing wings are increasingly studied for improving aerodynamic efficiency and flight adaptability in UAV systems. This has been previously unstudied as FishBAC wings have only been tested with stringers oriented at 90° to the spine for simplicity. On the other hand, this study introduces angled stringers inspired by the oblique nature of fish bones. For the testing of this novel string orientation, a NACA0012 airfoil was used. The profile was evaluated in terms of maximum total deformation and peak von Mises stress. Static structural simulations were performed using ANSYS Mechanical. Static loads were applied to the wing profile in the negative y-direction to simulate the deformation that actuators would cause. The angled configuration achieved 4.3% greater trailing-edge deflection than the conventional 90° stringer configuration, and peak von Mises stresses increased by 14.5%, but peak von Mises stresses remained below 5.2 MPa, well within the assumed 36 MPa yield limit, indicating a large structural safety margin. The angled stringers also exhibited 4.1% lower actuation stiffness, implying that lower force and energy can elicit the same deflection. Overall, the implementation of angled stringers onto FishBAC morphing wings improved actuation efficiency while preserving structural safety. Beyond advancing FishBAC technology, the results can inform the design of new energy-efficient UAVs as they establish stringer orientation as a potential design parameter for FishBAC morphing wings.

KEYWORDS: Engineering, Aerospace Engineering, Morphing Wing Structures, FishBAC Mechanism, Stringer Orientation.

Nomenclature

Symbol/Abbreviation	Meaning
ABS	Acrylonitrile Butadiene Styrene
F	applied force
F_{req}	required actuation force
FishBAC	Fish Bone Active Camber morphing mechanism
k	actuation stiffness
NACA	National Advisory Committee for Aeronautics
SF	safety factor
TPU	Thermoplastic Polyurethane
UAV	Unmanned Aerial Vehicle
U_{req}	required actuation energy
δ_{TE}	trailing-edge displacement
δ^*	prescribed camber displacement
σ	von Mises stress
σ_Y	material yield strength
σ_{Max}	maximum stress

Introduction

Background on Morphing Wings:

The history of aviation has long been tied to inspiration from natural flyers. Early pioneers in the area, such as Wilbur Wright, studied how birds maintained lateral balance to perform lateral turns and adapted this strategy into the first functional aircraft.[1] To this day, birds, shaped by millions of years of evolutionary refinement, continue to inspire new approaches to efficient flight. However, it is important to note that nature not only influences aeronautics based on avian flight. Certain principles based on hydrodynamics also influence the field of aviation. For instance, the fuselage of the Bayraktar Akıncı UAV resembles the body of a whale. Furthermore, structures like fish skeletons have also informed morphing concepts such as the Fish Bone Active Camber (FishBAC), which features an arrangement of stringers into an airfoil for trailing edge deflection to take place without hinged mechanisms being present on the surface of a wing.

Most morphing wings differ from wings with conventional control surfaces with hinged mechanisms, such as flaps and ailerons. This is because most morphing wings rely on a continuous structural deformation rather than the discrete hinges that cause discontinuities in the smooth wing profile. Therefore, morphing wings can improve aerodynamic efficiency, reduce drag, and minimize noise. While morphing technologies have been demonstrated in research, including NASA's Adaptive Compliant Trailing Edge (ACTE) and TU Delft's SmartX, their large-scale adoption in commercial aircraft remains limited due to the stringent demands of passenger aviation regarding safety.[2,3] In contrast, unmanned aerial vehicles (UAVs) present a practical testbed for such innovations, providing a low-cost, lower-risk platform to evaluate new technologies like morphing wings.[4,7] Therefore, the modeling of the FishBAC

DOI: 10.36838/IJHSR815.33

wing profile in this research was done for implementation on small-scale UAVs rather than large-scale aircraft.

Beyond avian inspiration, aquatic biomimicry also significantly informs aerospace design. Among various morphing concepts, the FishBAC design has emerged as a promising solution for trailing-edge morphing. FishBAC consists of a spine connected to multiple stringers covered by a flexible skin. When actuated by servo motors or actuators, the spine bends and transmits deformation through the stringers, producing a smooth deformation of the wing section while maintaining the smooth surface of the wing.[5]

However, in all published research regarding the FishBAC morphing wing, the stringers are oriented perpendicularly (90°) to the spine. For instance, at the University of Bristol, a model of a FishBAC profile is used, using a standard 90° configuration.[6] This assumption simplifies design and analysis, but it does not accurately reflect the biological structure it takes inspiration from, which is fish bones.

Literature Review on Morphing Wing Technologies:

The phrase "morphing" refers to continuous changes in wing geometry during flight, enabling a single airfoil profile to operate near-optimally across very different mission phases such as take-off, landing, and cruise.[2] Therefore, all significant changes in shape that can be observed from the outside of an aircraft can be labeled as a "morphing" structure.[3] Morphing UAV wings in the literature are analyzed in three different categories as shown in Figure 1, Planform morphing, out-of-plane morphing, and airfoil morphing.

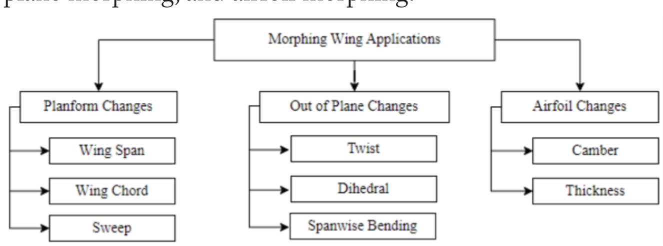

Figure 1: Classification of morphing wings.[7]

Note. This diagram categorizes morphing wing concepts into three primary groups: planform changes, out of plane changes, and airfoil changes.

Planform morphing involves dynamically changing a wing's three-dimensional shape to suit different phases of flight. This optimization can significantly improve the efficiency of aircraft. For example, the GNATSpar achieved a 20% span increase in wind tunnel tests, leading to improved aerodynamic efficiency.[8] Another example is the Transformer UAV, where it demonstrated a 39.1% increase in endurance and a 9.1% improvement in range with up to 50% span extension.[9] While chord morphing is less common, it has been applied in UAVs and rotorcraft through mechanisms like sliding ribs or expandable structures that enlarge the surface area of the wing during low-speed flight. Lastly, sweep morphing, done by changing sweep angle, has also been repurposed for UAV use. A notable example is a variable-sweep UAV with a +30° forward sweep that achieved final approach speeds under 3 m/s, well below its 9 m/s stall speed, enabling controlled low-speed landings.[10]

Out-of-plane morphing refers to modifications in a wing's orientation or curvature across three dimensions, without significantly altering its planform area.[2] Examples for out-of-plane changes include twist, dihedral, and spanwise bending, each of which aims at enhancing control and reducing aerodynamic loads for the aircraft.

These morphing modes are typically realized through structural components such as torque rods, servo-gearboxes, distributed ribs, compliant or membrane skins, and smart materials like shape-memory alloys (SMAs), which facilitate controlled bending.[11] Twist morphing, which is the earliest form of out-of-plane adaptation, was primarily employed by the Wright Brothers on the Wright Flyer to achieve roll control.[12,13] In this method, the local angle of incidence along the wingspan is adjusted, which improves maneuverability without the need for large geometric changes. Recent advances have demonstrated both active and passive twist implementations. For instance, lattice-based ultralight wings have exhibited aeroelastic twist capabilities, with wind tunnel testing at NASA Langley confirming a 46% reduction in global bending stiffness and a 43% reduction in torsional stiffness, alongside an improved lift-to-drag ratio.[3]

Dihedral morphing involves altering the upward or downward tilt of the wings, either globally or in localized sections, to achieve aerodynamic stability. Mechanisms such as gull-wing configurations with independently actuated inner and outer panels, or hinge-mounted folding wingtips, have been developed for this purpose. An example that is worth noting is the work by Abdulrahim and Lind.[3] They tested a small UAV that included actuated inner and outer panels, which was able to achieve ±40° variation in dihedral angle.[14] This system enabled improved sideways control, which ultimately demonstrated that dihedral morphing can effectively supplement or even replace traditional aileron systems in lightweight aircraft. Lastly, spanwise bending, which mimics the backward curve of bird wings, is used to optimize lift distribution and reduce structural loads without having to alter the wing planform. The Hyperelliptical Cambered Span (HECS) wing exemplifies this approach, employing SMA wires to induce controlled curvature.[15] It has achieved measurable reductions in drag coefficient at moderate angles of attack and is considered complementary to trailing-edge morphing systems like FishBAC, where spanwise bending handles load optimization, while FishBAC adjusts camber and control authority.[3]

Airfoil-level morphing works to preserve a smooth aerodynamic surface, reducing drag and noise while improving efficiency. A landmark example is NASA and AFRL's Adaptive Compliant Trailing Edge (ACTE) project, which successfully flight-tested smooth, flexible flaps on a Gulfstream G-III and confirmed benefits in lift modulation and aeroacoustics.[16] Among modern designs, the Fish Bone Active Camber (FishBAC) system has emerged as a particularly promising structure for small UAVs. The FishBAC structure is composed of a spine and flexible skin and multiple stringers oriented at 90° to the spine. A distinguishing feature of FishBAC is that it produces large and continuous shape changes without any smoothness being lost on the surface of the airfoil. For example, a rib-sliced morphing wing flight-tested on a Talon UAV reported a 14.1% improvement in flight efficiency versus its conventional wing; this result is reported in a 2023 review that summarizes the primary study.[17]

FishBAC is a compliant trailing-edge morphing architecture that changes airfoil camber smoothly, without discrete hinges or surface gaps.[18] Structurally, a bending “spine” carries a set of spanwise stringers that support an elastomeric skin, and tendons impose bending moments to morph the trailing edge.[14] Woods and Friswell introduced this concept, and have since been refined and tested in multiple wind-tunnel campaigns, showing clear efficiency advantages over comparable hinged flaps.[3] More recent investigations have also emphasized the aerodynamic benefits of compliant morphing concepts for load control and drag reduction.[19] However, as mentioned before, current FishBAC models simplify the fish bone structure. A diagram showing a skeletal image of a fish in Figure 2 illustrates the oblique nature of fish bones.

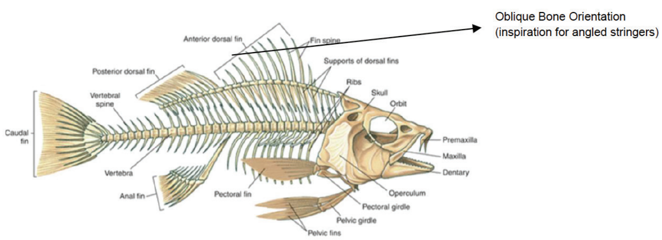

Figure 2: Diagram showing the skeletal image of a fish.[19]

Note. This diagram illustrates the spine, ribs, and supporting structures that inspired the FishBAC configuration. The alignment of the fish bones provides the biological basis for the flexible and load-bearing abilities of the FishBAC wing design, shown by the arrow.

Early FishBAC studies established strong aerodynamic benefits. Bench-scale and quasi-2D tests reported greater than or equal to 16% improvements in lift-to-drag ratio across the full lift range and greater than 50% gains at moderate to high lift coefficients, while control authority of ΔCL of roughly 0.72 was demonstrated relative to a plain flap.[18] More recent modular implementations using 3D-printed TPU skins achieved ΔCL of roughly 0.55 with minimal drag penalties, confirming the concept’s suitability for UAV-scale wings where weight and actuation efficiency are critical.[17]

Research Gap:

Currently, all FishBAC implementations have oriented the stringers perpendicularly (90˚) to the main spine for simplicity in testing; however, it is important to note that this does not reflect what exists in nature. Although a precise quantitative range for bone angles was not located in the literature, skeletal anatomy diagrams, such as those in Figure 2, clearly show that the bones emerge at non-perpendicular angles, typically oblique relative to the spine. The angles at which the bones emerge are usually said to be between 30-75˚ to the horizontal. From this biological range, 60˚ was chosen as a mid-range angle to represent an oblique structure while allowing a clear comparison with the traditional 90˚ configuration.

Research Question and Motivations:

While the angled configuration is inspired by fish skeletons, their function in fish is not the same as in the FishBAC system. Fish move by bending side-to-side, whereas FishBAC bends up and down. Therefore, this study does not assume a direct biological equivalence, but instead uses the angled structure as a source of inspiration for potentially improved load distribution and flexibility.

This study, therefore, addresses the following research question: Can introducing angled stringers (60˚ orientation) into a FishBAC morphing wing improve structural deformation performance and actuation efficiency compared to the conventional 90˚ stringer configuration?

This question arises because in fish skeletons, supporting bone structures branch from the spine at oblique angles rather than perpendicular ones, suggesting that angled structural stringers may distribute loads more efficiently.

The motivation of this study is therefore to investigate whether a biomimetic stringer orientation can improve morphing performance while maintaining safe structural stress levels. By comparing angled and perpendicular stringer configurations under identical loading, this research aims to provide insight into whether bioinspired structural geometry can enhance the efficiency of FishBAC morphing wings for UAV applications. However, this study is limited to static structural simulations and does not capture the full aerodynamic-structural interaction that may occur in real morphing wings, which should be investigated in future experimental or fluid-structure interaction studies.

Methodology for CAD Design

This investigation was carried out using ANSYS Workbench software. The methodology was designed to provide a comparison between both the angled stringer configuration, Figure 4, and the conventional 90˚ stringer configuration, as shown in Figure 3. This comparison was made possible by controlling boundary conditions, materials, and meshing across both configurations. Therefore, the study safely ensures that the difference in stringer orientation can account for all recorded differences.

The FishBAC airfoil configurations were modelled in ANSYS SpaceClaim by using a standardized NACA 0012 airfoil profile as a basis. This profile was imported from a DAT coordinate file. It was chosen because it is widely used in morphing-wing research due to its symmetric nature.

Each model was defined with a 100 mm chord length and 100 mm span, with no other type of morphing strategy as listed in the literature review utilized. While the FishBAC was designed for small-scale UAV use, these chosen dimensions were not intended to replicate a full-scale UAV wing, but rather a scaled structural section. The utilization of this smaller geometry reduced computational cost while still preserving realistic proportions for the spine, stringers, and skins.

Both configurations were made sure to adhere to the same general FishBAC composition, consisting of a rigid leading-edge comprising the forward 20 mm of the chord, a spine that extends alongside the trailing edge, and sixteen stringers,

DOI: 10.36838/IJHSR815.33

angled or perpendicular depending on the configuration, to support the trailing edge beneath upper and lower skins. The stringers were evenly distributed at 2.5 mm intervals along the chord between the spine and the trailing edge, which provided uniform structural support and allowed deflection to occur smoothly across the morphing region.

For both configurations, the stringers were modeled with a uniform thickness of 0.5 mm, while the spine was given a 1.0 mm thickness. The upper and lower skins were each assigned a 0.5 mm thickness, chosen to strike a balance between flexibility and the need to resist local buckling. The FishBAC structure incorporated 16 internal stringers distributed evenly between the upper and lower surfaces (8 per surface) to provide symmetric structural support.

Finally, the Share Topology mode was enabled in SpaceClaim to mesh all components, ranging from the spine, stringers, and skins to the rigid leading edge, to mesh as a single continuous body. Figure 3 shows a 90° configuration of the FishBAC design, while Figure 4 shows the 60° configuration.

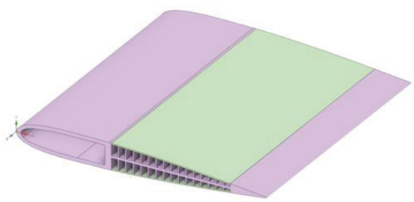

Figure 3: FishBAC 90° configuration isometric view taken on ANSYS SpaceClaim.

Note. This configuration uses stringers oriented perpendicular to the FishBAC spine, which represents the traditional baseline used in previous studies.

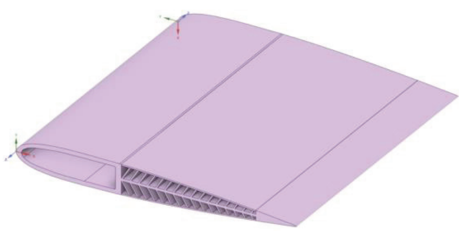

Figure 4: FishBAC 60° configuration isometric view taken on ANSYS SpaceClaim.

Note. This configuration uses stringers oriented at 60° to the spine.

For the material selection of the FishBAC, two different materials were assigned to both configurations. The skeleton, which includes the leading-edge section, the spine, and the stringers, was modeled using high-impact acrylonitrile butadiene styrene (ABS). ABS is a widely used thermoplastic that is available in the ANSYS materials library. Its mechanical properties are summarized in Figure 5. The choice of utilizing ABS for the stiff areas of the wing was motivated by its prior use in morphing wing studies, where it demonstrated an ideal stiffness for structural integrity to be preserved throughout testing.[21]

Additionally, the upper and lower skins were modeled with a hyperelastic Mooney-Rivlin, using thermoplastic polyurethane (TPU) as the base material. Values for this plastic had to be manually entered into the ANSYS material library because the values were not present in the library. TPU was selected because it is both lightweight and capable of sustaining large elastic deformations. The mechanical properties for TPU, which include Young's modulus and density, were taken from supplier datasheets (Figure 6a). In contrast, while additional values missing from these datasheets were gathered from technical plastics suppliers such as Plastore (Figure 6b). Although Poisson's ratio was not explicitly reported in the datasheet, values from commercial TPU products such as Desmopan® indicate a range of 0.45-0.50.[22] Ultimately, a representative value of 0.45 was adopted in this study. Using these inputs, ANSYS automatically calculated the corresponding bulk modulus and shear modulus for the material.

It is important to note that while both ABS and TPU exhibit nonlinear behavior under large strains. However, nonlinear effects were intentionally disabled in this study. This decision was made because nonlinear simulations are significantly more computationally expensive and can lead to solver instabilities, which were faced during preliminary trials while attempting to analyze the behavior of the wing profile under load. Using linear elastic models for both materials ensured that differences in deformation, strain energy, and stress could be attributed solely to the orientation of the stringers.

Property	Value	Unit
Material Field Variables	Table	
Density	1030	kg m^-3
Isotropic Secant Coefficient of Thermal Expansion		
Coefficient of Thermal Expansion	0.000184	C^-1
Isotropic Elasticity		
Derive from	Young's Modulus and Poisson...	
Young's Modulus	1.628E+09	Pa
Poisson's Ratio	0.4089	
Bulk Modulus	2.9784E+09	Pa
Shear Modulus	5.7776E+08	Pa
Tensile Yield Strength	Tabular	
Tensile Ultimate Strength	Tabular	

Figure 5: Material properties of ABS (high-impact) plastic in the ANSYS library.

Note. The figure shows the material properties of ABS plastic, including density and isotropic elasticity values.

Property	Value	Unit
Material Field Variables	Table	
Density	Tabular	
Scale	1	
Offset	0	kg m^-3
Isotropic Elasticity		
Derive from	Young's Modulus and Poisson...	
Young's Modulus	20.684	MPa
Poisson's Ratio	0.45	
Bulk Modulus	6.8948E+07	Pa
Shear Modulus	7.1325E+06	Pa

Figure 6: a. Material properties of manually entered TPU in the ANSYS library.

Note. The figure shows the material properties of TPU plastic such as young's modulus, poisson's ratio, bulk modulus and shear modulus.

Typical Properties of Elastollan®	ASTM Test Method	Units	Typical Values
All the physical properties reported here are measured on injection molded samples. Properties of sheet or film samples of this product are also available upon request.			
Specific Gravity	ASTM D 792	g/cm³	1.19
Shore Hardness	ASTM D 2240	Shore A or D	85A
Taber Abrasion	ASTM D 1044	mg loss	25
DIN Abrasion	DIN 53516	mm³ loss	25
E-Modulus	ASTM D 412	psi	3000
Flexural Modulus	ASTM D 790	psi	3600
Tensile Strength	ASTM D 412	psi	6000
Tensile Stress at 100% Elongation	ASTM D 412	psi	1000
Tensile Stress at 300% Elongation	ASTM D 412	psi	2200
Ultimate Elongation	ASTM D 412	%	590
Tear Strength	ASTM D 624, Die C	lb/in	620
Compression Set 22h at 70°C 22h at 23 °C	ASTM D 395 "B"	% of original deflection	35 25
Glass Transition temperature*	BASF Analytical Method	°C	-40
Vicat Softening Temperature	ASTM D 1525	°C	110
DMA Softening Temperature	BASF Analytical Method	°C	100

Figure 6: Material properties for Elasollan TPU. [23]

Note. The figure shows the material properties for Elasollan TPU plastic, which were entered into ANSYS library.

Using the automatic hexahedral-dominant meshing mode in ANSYS Mechanical, the FishBAC models were meshed. Figure 7 shows the details of the meshing approach. A global element size of 0.50 mm was used. This element size was chosen since the stringers' smallest structural part was also 0.50 mm thick. Preliminary mesh refinement trials confirmed mesh independence. Element sizes below 0.50 mm resulted in less than 2% variation in peak von Mises stress, indicating sufficient numerical convergence. This guaranteed that at least one finite element was made across the thickness of each part. This is highly important for getting realistic bending and stress distributions.

When CAD modeling was done, Share Topology was turned on, so all the pieces of the FishBAC structure, the spine, stringers, skins, and rigid leading edge, were meshed as one continuous body. The mesh that came out of this was mostly made up of 20-node hexahedral elements (Hex20), with 15-node wedge elements (Wed15) added in places where geometry required changes.

Figure 8 and Figure 9 show meshed images of FishBAC, showing perpendicular stringer orientation and angled stringer orientation, respectively.

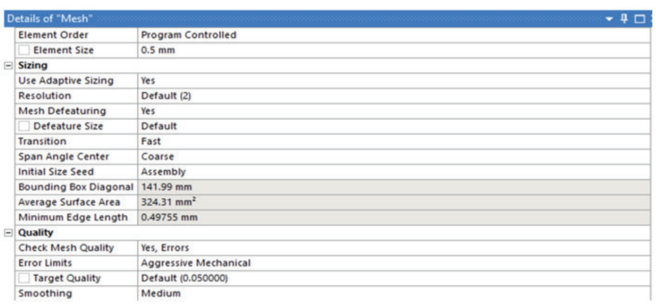

Details of "Mesh"	
Element Order	Program Controlled
Element Size	0.5 mm
Sizing	
Use Adaptive Sizing	Yes
Resolution	Default (2)
Mesh Defeaturing	Yes
Defeature Size	Default
Transition	Fast
Span Angle Center	Coarse
Initial Size Seed	Assembly
Bounding Box Diagonal	141.99 mm
Average Surface Area	324.31 mm²
Minimum Edge Length	0.49755 mm
Quality	
Check Mesh Quality	Yes, Errors
Error Limits	Aggressive Mechanical
Target Quality	Default (0.050000)
Smoothing	Medium

Figure 7: Mesh settings on ANSYS Mechanical for angled configuration.

Note. The figure shows the settings that define the element size and quality parameters used to ensure consistent and accurate results for the structural simulations.

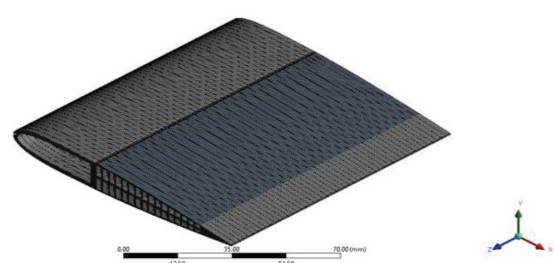

Figure 8: Mesh for FishBAC 90° configuration.

Note. The figure shows a mesh applied to the 90° *configuration.*

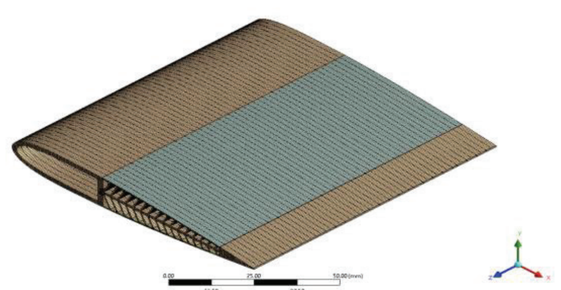

Figure 9: Mesh for FishBAC *60°* configuration.

Note. The figure shows a mesh applied to the 60° *configuration.*

Boundary conditions were used to determine the physical limits of a morphing wing section. The rigid leading-edge block was modeled as a fixed support, which meant that all degrees of freedom for translation and rotation were limited. This design made sure that deformation stayed in the flexible trailing-edge area and didn't spread to the part of the wing that didn't change shape. The exact location where this condition was applied can be seen in Figure 10.

Figure 11 shows where the forces that caused the deformation were applied at the trailing edge. These stresses were represented as surface loads, which is how they would work in a real morphing wing, because the actuation forces are spread out across a region rather than being applied at one spot. The load sizes (ranging from 5 N to 7 N) were determined after preliminary tests that showed that they were big enough to cause noticeable deflections.

Figure 10: Fixed support condition for 60° configuration.

Note. The purple area depicts where fixed support was applied.

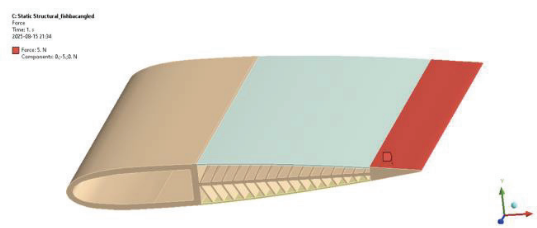

Figure 11: Position of load application at the trailing edge.

Note. The red area depicts where loads were applied.

All simulations were performed in ANSYS Workbench (Static Structural module). A linear-elastic solver was utilized. A total of six simulations were conducted: three simulations for the perpendicular (90°) configuration and three for the angled (60°) configuration. Four output variables were extracted for each run, with only von Mises stress and total deformation being utilized for this research.

- Directional deformation in the Y-axis, representing trailing-edge compliance.
- Total deformation magnitude is used to confirm that displacement occurred primarily in the load direction.
- Strain energy indicates how much elastic energy was stored during deformation.
- Equivalent (von Mises) stress, identifying peak stress levels for comparison against material strength.

Results and Discussion

Deformation:

Total deformation values were analyzed. Table 1 summarizes the maximum trailing-edge deflections for both configurations. The angled (60°) stringers consistently produced approximately 4.3% greater deformation than the perpendicular

DOI: 10.36838/IJHSR815.33

(90°) baseline at each load. This result highlights the role of directional compliance introduced by oblique stringers. While perpendicular stringers resist bending directly by transferring loads vertically into the spine, angled stringers resolve a portion of the applied force along their axis. This redistribution allows larger deflections under the same load.

Table 1: Deformation in the y-axis for both angled configurations.

Note. Directional deformation in the y-axis for loads 5 N, 6 N, and 7 N, and percentage change in deformation.

Load (N)	90° Max Deformation (mm)	60° Max Deformation (mm)	% Change
5	4.5945	4.7929	4.32%
6	5.5135	5.7515	4.32%
7	6.4324	6.7101	4.32%

The percentage increase is the same for all loads because the simulation is linear, so deformation increases in direct proportion to the applied force. The angled FishBAC structure accommodates greater cambering deflection at the cost of higher stress concentrations. Images from total deformation analysis for 7 N, for both FishBAC configurations, can be seen in Figures 12 and 13, which show deformation analysis results for the 90° configuration and the 60° configuration.

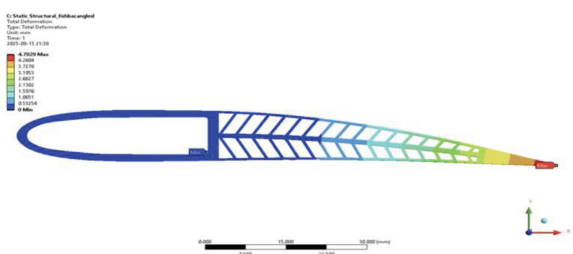

Figure 12: Total Deformation Analysis Results for 60° Configuration 2D.

Note. Sideways view of total deformation analysis results for 60° angled configuration when under the load of 7 N, taken on ANSYS Mechanical.

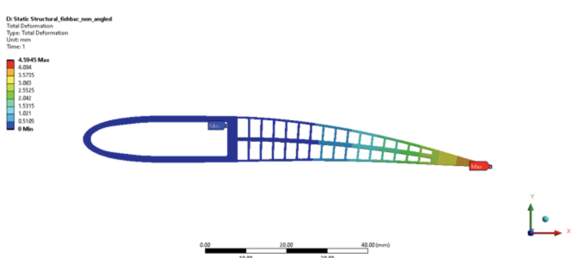

Figure 13: Total Deformation Analysis Results for 90° configuration 2D.

Note. Sideways view of total deformation analysis results for 90° angled configuration when under the load of 7 N, taken on ANSYS Mechanical.

Von Mises stress:

In the perpendicular design, stringers channel vertical loads directly into the spine, producing a relatively uniform stress distribution. In the angled configuration, however, the applied force is resolved into both axial and shear components along the stringers. This redistribution increases compliance but also introduces localized stress concentrations, particularly at the edges where stringers meet the spine and skins. The oblique orientation, therefore, creates additional bending moments and shear forces, increasing peak stresses despite the greater overall deformation.

This trade-off is different from patterns observed in fish skeletons. Instead, in biological systems, these stresses are mitigated by adaptations such as graded material properties and continuous remodeling naturally done by fish. In the FishBAC model, such mechanisms are absent, leaving junction points more vulnerable to concentrated stress.

Overall, the results highlight a clear design compromise. Angled stringers enhance compliance and actuation efficiency, but at the cost of increased localized stresses. For UAV morphing wing applications, this suggests that angled supports could be viable if paired with reinforcement or advanced materials at junctions to prevent premature structural failure. Table 2 shows that the angled (60°) configuration consistently generated approximately 14.5% higher maximum von Mises stress than the perpendicular (90°) baseline across all load cases.

Table 2: Von Mises stress for both configurations.

Note. Table showing maximum von Mises stress values for both FishBAC configurations and the percentage increase in maximum stress values for each load applied.

Load (N)	90° Max Stress (MPa)	60° Max Stress (MPa)	% Increase in maximum stress
5	3.2703	3.7434	14.47%
6	3.9244	4.4921	14.47%
7	4.5784	5.2408	14.47%

Once again, the percentage increase in maximum stress is the same because of the fact that linear analysis was conducted, as stress increases in direct proportion to force. For safety factor analysis, yield values were taken from literature sources to enable safety-factor calculations. Data compiled by MatWeb report ABS yield strengths in the range of 27-100 MPa, with common values falling between 40-45 MPa. To maintain a conservative margin, a value of 36 MPa was selected for calculations.

The safety-factor analysis was conducted as a screening check under linear elasticity using Equation (1). In this approach, peak von Mises stresses are compared directly against the assumed yield strength, under the simplifying assumption that the material remains linear up to yield. Safety factors were calculated using σ_Y = 36 MPa and are summarized in Table 3.

$$SF = \frac{\sigma_y}{\sigma_{max}} \tag{1}$$

Table 3: Safety factor values for both configurations.

Note. Table showing safety factor values for both FishBAC configurations for each load applied.

Load (N)	SF (90°)	SF (60°)
5	11.0	9.6
6	9.2	8.0
7	7.9	6.9

The table shows that in the worst case (7 N, angled configuration), the safety factor remains ~6.9. Thus, although angled stringers increased stress by 14.5%, the absolute values are well within safe limits. The main implication is not failure risk, but a design trade-off: increased compliance and efficiency come at the cost of higher local stresses at stringer-spine junctions.

Strain Energy and Efficiency:

The performance of a morphing trailing-edge concept can be evaluated by how much actuator effort is required to achieve a target camber. In practice, UAV servos are torque-limited rather than energy-limited; thus, the critical efficiency metric is the force and energy required to reach the same trailing-edge displacement.

In linear static mechanics, actuation stiffness is defined in Equation (2)

$$k = \frac{F}{\delta_{TE}} \tag{2}$$

where F is the applied force and δ_{TE} is the trailing-edge displacement for a prescribed camber δ^*. The actuator demands relate directly to stiffness, as shown in Equation (3):

$$F_{req} = k\delta^* \tag{3}$$

$$U_{req} = \frac{1}{2}k\delta^{*2} \tag{4}$$

The simulations showed that the angled (60°) FishBAC had an average stiffness of 1.043 N/mm compared to 1.088 N/mm for the perpendicular baseline. All values for stiffness were the same because linear analysis was conducted. This 4.1% reduction in stiffness means that to achieve the same target camber, the angled configuration requires 4.1% less actuation force and therefore 4.1% less actuation energy. Since the same camber displacement δ^* is prescribed, the reduction in stiffness produces an equivalent reduction in actuation force and strain energy.

The reduction in structural stiffness directly decreases the strain energy required for actuation. Because actuation energy is proportional to stiffness according to Equation (4), the 4.1% reduction in stiffness translates to an equivalent reduction in actuator work required to achieve the same camber displacement. This improvement could reduce servo torque requirements and increase overall UAV efficiency.

From a design standpoint, the angled configuration's lower stiffness directly benefits UAV-scale morphing wings, where servos are limited in torque and battery current. Achieving the same camber with ~4% less force reduces actuator sizing requirements and decreases hold current during trimmed flight. This mirrors biological skeletons: angled fin rays and rib structures store elastic energy and enhance flexibility, reducing muscular effort for a given motion. In UAV applications, the same principle translates to lighter actuation systems and potentially longer endurance.

Discussion:

This study aimed to examine how changing the stringer orientation of a FishBAC wing structure from perpendicular to the spine to a 60-degree angle configuration would affect the structural performance of the FishBAC morphing wing. This work provides the first quantitative assessment of adopting a biologically inspired angled arrangement. The goal was to determine whether a biologically inspired configuration (which pertains to the configuration with 60° angles) could improve actuation efficiency without compromising safety limits.

The results indicate that the configuration with the angled stringers enhanced maximum trailing edge deflection by 4.3% for all loads applied. This is important because it confirms that oblique stringers increase the compliance of FishBAC when faced with loads. This suggests that the loads are resolved along the axis to contribute to greater deformation in the y-axis. Additionally, a reduction of 4.3% in stiffness was observed, which indicates that less actuator/servo motor force and energy are needed to achieve a particular amount of deflection in the angled configuration in comparison to the perpendicular one. This is an important advantage for UAVs that possess servo motors or actuators that can only deliver a specific amount of torque due to energy constraints caused by battery size. However, these improvements also brought along a 14.5% rise in local stress, which was concentrated in the locations where the spine and stringer converged. Despite this increase, the stress remained below the ABS yield limit, which ensures structural safety for the angled configuration regardless.

Lastly, for a morphing wing, the goal is to achieve the required deformation using less actuation force while keeping stresses within safe limits. From this perspective, the angled configuration can be considered an improvement, as it reduces stiffness and increases trailing-edge deflection, while all stress values remain below the material yield limit.

Limitations and Future Directions:

Firstly, given that this research aimed to examine the effects of an angled configuration of FishBAC on its structural performance, rather than its aerodynamic performance, a static structural analysis was used rather than a CFD analysis. In the future, using CFD can capture aerodynamic loads and therefore provide a more realistic view into how the airfoil will perform in the air. Additionally, another set of limitations was the absence of non-linear effects and a small-scale design. Such limitations were present because of technical reasons, where the computer couldn't process CFD and non-linear effects. Furthermore, this study used a linear static analysis, assuming steady loading conditions. Static analysis assumes steady-state loading, whereas real morphing wings experience dynamic actuation cycles. Fatigue analysis would be valuable for flight-ready designs. Moreover, future work should focus on modelling the angled configuration at larger scales, such as for medium-sized UAVs. This will be beneficial because UAVs of a larger scale can benefit significantly from the energy efficiency that FishBAC morphing wings elicit, both aerodynamically and structurally. Importantly, future work should explore more stringer angles (e.g., 45°, 60°, 75°) to determine optimal configurations for different UAV's. Additionally, fish possess the ability to remodel bone tissue in response to stress. Morphing structures currently lack this capability, which introduces an opportunity for the future use of adaptive materials in morphing wing designs. Lastly, a physical model testing of the FishBAC with an angled configuration could also be carried out.

DOI: 10.36838/IJHSR815.33

Conclusion

This study investigated how altering the orientation of stringers in a FishBAC morphing wing influences structural performance. Specifically, a biomimetic configuration with 60° angled stringers was compared to the conventional 90° configuration using simulations in ANSYS.

The results demonstrated that the angled configuration increased trailing-edge deflection by 4.3% while reducing actuation stiffness by 4.1%, indicating that less actuator force is required to achieve the same camber. However, the angled structure also produced 14.5% higher peak von Mises stresses, primarily concentrated at stringer-spine junctions.

Despite this increase, safety-factor calculations confirmed that stresses remained well below the ABS yield strength, indicating that the configuration is structurally viable for UAV-scale morphing wings.

In summary, angled stringers introduce a measurable trade-off between compliance and stress but ultimately demonstrate a feasible path toward more adaptive and efficient morphing-wing designs. These findings suggest that adopting angled stringers can make small-scale UAV morphing wings lighter and more energy-efficient by lowering the actuation demand for the deformation required for the morphing wing.

Future research could incorporate more stringer angles to determine optimal configurations for different UAV's. Importantly, since fish have the ability to change how their bone tissue responds to stress, a further study could attempt to incorporate this through the use of adaptive materials or special algorithms connected to actuators.

Acknowledgments

I would like to sincerely thank Gamze Kaynak for her constant support and motivation throughout this research, and to Baykar Technologies for providing access to the ANSYS software and computers.

References

1. NASA Glenn Research Center. (2023, January 21). *Wright Brothers' aircraft.* https://www1.grc.nasa.gov/beginners-guide-to-aeronautics/wright-brothers-aircraft/
2. Ajaj, R. M., Friswell, M. I., Bourchak, M., & Harasani, W. (2021). *Recent developments in the aeroelasticity of morphing aircraft*. Progress in Aerospace Sciences, 120, 100682. https://doi.org/10.1016/j.paerosci.2020.100682
3. Barbarino, S., Bilgen, O., Ajaj, R. M., Friswell, M. I., & Inman, D. J. (2011). *A review of morphing aircraft*. Journal of Intelligent Material Systems and Structures, 22(9), 823–877. https://doi.org/10.1177/1045389X11414084
4. Cheng, G., Ma, T., Yang, J., Chang, N., & Zhou, X. (2023). *Design and experiment of a seamless morphing trailing edge*. Aerospace, 10(3), 282. https://doi.org/10.3390/aerospace10030282
5. Galantai, V. P. (2010). *Design and analysis of morphing wing for unmanned aerial vehicles* (Master's thesis, University of Toronto). https://utoronto.scholaris.ca/server/api/core/bitstreams/30564380-2afe-4f43-9836-0f74ffe9437c/content
6. Szyszko, S. (2022). *Feasibility of FishBAC morphing camber technology in fixed-wing UAV applications* (Doctoral thesis, University of Bristol). https://research-information.bris.ac.uk/ws/portalfiles/portal/388605139/PGR_submission_szyszko_szymon_1984156.pdf
7. Ozbek, E., Ekici, S., & Karakoc, T. H. (2023). *Unleashing the potential of morphing wings: A novel cost-effective morphing method for UAV surfaces, rear spar articulated wing camber*. Drones,7(6), 379. https://doi.org/10.3390/drones7060379
8. Ajaj, R. M., Friswell, M. I., Bourchak, M., & Harasani, W. (2016). *Span morphing using the GNATSpar wing*. Aerospace Science and Technology, 53, 38–46. https://doi.org/10.1016/j.ast.2016.03.009
9. Ajaj, R. M., & Jankee, G. K. (2018). *The transformer aircraft: A multimission unmanned aerial vehicle capable of symmetric and asymmetric span morphing*. Aerospace Science and Technology, 76, 512–522. https://doi.org/10.1016/j.ast.2018.01.022
10. Greatwood, C., Waldock, A., & Richardson, T. (2017). *Perched landing manoeuvres with a variable sweep wing UAV*. Aerospace Science and Technology, 71, 510–520. https://doi.org/10.1016/j.ast.2017.10.012
11. Tavares, S. M. O., Gamboa, P. V., & de Castro, P. M. S. T. (2025). *Aircraft wings and morphing: Evolution of the concepts*. Encyclopedia, 5(3), 101. https://doi.org/10.3390/encyclopedia5030101
12. Smithsonian Education. (n.d.). *Stories of the Wrights' flight*. https://www.smithsonianeducation.org/educators/lesson_plans/wright/wing_warping.html
13. Abdulrahim, M., & Lind, R. (2004). *Flight testing and response characteristics of a variable dihedral morphing UAV*. AIAA Atmospheric Flight Mechanics Conference. https://doi.org/10.2514/6.2004-5113
14. Woods, B. K. S., & Friswell, M. I. (2014). *Preliminary investigation of a fish bone active camber morphing concep*t. Journal of Intelligent Material Systems and Structures, 25(12), 1512–1524. https://doi.org/10.1177/1045389X13485859
15. Miller, E. J., Griffin, C. F., Violette, C. J., & Kota, S. (2015). Approach for structurally clearing *an adaptive compliant trailing-edge flap for flight*. Society of Flight Test Engineers Symposium. NASA. https://ntrs.nasa.gov/citations/20150019727
16. Rivero, A. E., Fournier, S., Heeb, R. M., & Woods, B. K. S. (2022). *Design, manufacture, and wind-tunnel test of a modular FishBAC wing with novel 3D-printed skins*. Applied Sciences, 12(2), 652. https://doi.org/10.3390/app12020652
17. Rivero, A. E., Fournier, S., Woods, B. K. S., & Friswell, M. I. (2021). *Experimental aerodynamic comparison of active camber morphing and trailing-edge flaps*. AIAA Journal, 59(7), 2627–2640. https://doi.org/10.2514/1.J059867
18. Royal Aeronautical Society. (n.d.). *Shape shifters*. https://www.aerosociety.com/news/shape-shifters/
19. GeeksforGeeks. (2025, July 23). *Skeletal system of fish*. https://www.geeksforgeeks.org/biology/skeletal-system-of-fish/
20. Nguyen, K., Yu, N., Bandi, M. M., Venkadesan, M., & Mandre, S. (2017). *Curvature-induced stiffening of a fish fin*. Journal of the Royal Society Interface, 14(130), 20170247. https://doi.org/10.1098/rsif.2017.0247
21. van Mkhoyan, A., van Tooren, M., & de Breuker, R. (2022). *SmartX: Modular morphing wing design using integrated and distributed trailing-edge morphing*. Smart Materials and Structures,31(12), 125025. https://doi.org/10.1088/1361-665X/ac9d8b
22. Covestro AG. (n.d.). *Mechanical properties of Desmopan® and Texin®*. https://solutions.covestro.com/en/highlights/articles/theme/product-technology/mechanical-properties-tpu
23. Plastore S.R.L. (n.d.). *Hard trading: The only Italian outlet for thermoplastic granules*. https://plastore.it/

Authors

Derin Bahşiş is a senior in the International Baccalaureate program at the Koç School in Istanbul, Turkey. Her areas of interest include morphing wing technology, bio-inspired engineering, and sustainable engineering design. Outside of academics, she currently leads the Koç Aviation Club at her school and teaches biomimicry workshops to students across many cities. Also, she is an avid bird watcher.

Zehra Sena Şentürk graduated from the University of Samsun with a Bachelor's degree from the Department of Aerospace Engineering in 2024. She started working as an R&D engineer at Baykar Technology in October 2023. After that, she started a master's degree at Istanbul Technical University, Department of Aeronautical and Astronautical Engineering, and she is still pursuing it. Her research interests include gas turbine engines, thermodynamics, space technology, energy, and aerodynamics.

DOI: 10.36838/IJHSR815.33